# Numerical and Neural Network Analysis of Natural Convection from a Cold Horizontal Cylinder above an Adiabatic Wall

A. R. Tahavvor [†] and M. Nazari

*Department of Mechanical Engineering, Shiraz Branch, Islamic Azad University, Shiraz, Iran*

†*Corresponding Author Email: tahavvor@iaushiraz.ac.ir*

## ABSTRACT

Free convection around cold circular cylinder above an adiabatic plate at steady-state condition has been investigated both numerically and by artificial neural networks. There is a growing demand for a better understanding of free convection from a horizontal cylinder in the areas like air cooling, refrigeration and air conditioning system, etc. Governing equations are solved in some specified cases by finite volume method to generate the database for training the neural network in the range of Rayleigh numbers of $10^5$ to $10^8$ and a range of cylinder distance from adiabatic plate (L/D) of 1/4, 1/2, 1/1, 3/2 and 4/2, thereafter a Multi-Layer Perceptron network is used to capture the behavior of flow and temperature fields and then generalized this behavior to predict the flow and temperature fields for other Rayleigh numbers. Different training algorithms are used and it is found that the back-propagation method with Levenberg-Marquardt learning rule is the best algorithm regarding the faster training procedure. It is observed that ANN can be used more efficiently to determine cold plume and thermal field in less computational time and with an excellent agreement. From obtained results, average Nusselt number of the cylinder investigated to study the effect of adiabatic wall on the isothermal cylinder. It also observed that in spaces farther than L/D = 3/2, average Nusselt number is almost constant, so the affect is renouncement and it works like a cylinder in an infinite environment.

Keywords: Natural convection; Cold horizontal cylinder; Artificial Neural Network; Adiabatic wall.

## 1. INTRODUCTION

In this research a numerical methods and neural network analysis are used for two-dimensional laminar free convection from an isothermal cold circular horizontal cylinder above an adiabatic plate under steady state that is used in the many applications such as energy storage systems, air conditioning, air cooling, solar heating and cooling, natural circulation, etc. Previous investigations used different kinds of methodologies for the hot cylinder, while hear the case studied when the temperature of the cylinder surface is below the surrounding one.

Artificial neural networks originate from the works of McCulloch and Pitts (1990) who demonstrated the ability of interconnected neurons to calculate some logical functions. For further detail analysis, to reduce cost of studies and saving computational time, soft programming methods new approaches such as Artificial Neural Networks can be an alternative and a new attempt. Artificial Neural Networks have been used by various researchers for modeling and predictions in the field of energy engineering systems.

The most important problems in engineering applications such as heat exchangers, boiler design and air cooling systems for air conditioning are study of natural convection heat transfer. Natural convection heat transfer from a horizontal cylinder has been studied numerically and experimentally for over 50 years but it is reported by the researchers (Atayılmaz *et al.* 2010) that the obtained results show high levels of deviation among each other due to various reasons. Yamamoto *et al.* (2004) studied Natural convection around a horizontal circular pipe coupled with heat conduction in the solid structure. One of the foremost studies on the neural networks took place by Thibault *et al.* (1991). They introduced the artificial neural networks and solved three problems by this method to prove that it has a complete and exact result. One of the best problems that could explain the competence of neural networks was solved by Heckel *et al.* They worked on the convection of the vertical cylinders. It was a complicated problem contained 32 parameters in nonlinear equations.

Recently, artificial neural networks are used to simulate and predict the behavior of computational and experimental mass/heat transfer phenomena (Temeyer *et al.* 2003; Hasiloglu *et al.* 2004; Varol *et al.* 2007) and for fluid flow (Firat and Goungor 2007). Saito *et al.* (1969) in several experiments for Grashof numbers of $2\times10^6$ to $3\times10^6$, investigate the effect of adiabatic plate above heated horizontal cylinder. Their results show that the rate of heat transfer is minimized when the ratio of cylinder distance from plate to its diameter is about 0.12.

Free convection heat transfer from the hot pipe below an isothermal surface for Rayleigh numbers of $10^3$ to $10^5$ and $1/10 < L/D < 1/2$ is studied by Lawrence *et al.* (1999). Results show that when the distance between pipe and surface is greater than the diameter of the pipe, the effect of the surface on the heat transfer rate of the pipe is negligible. They also report that Nusselt number increases for spacing of about $L/D = 1/4$.

In another study, Ashjaee *et al.* (2007) used an interferometer to investigate free convection from a cylinder below an adiabatic wall for Rayleigh numbers of 1000 to 40000. Their results show that for $L/D > 3/2$ the effect of the wall on cylinder heat transfer is negligible. These results are validated in similar investigations on free convection heat transfer from a horizontal circular cylinder (Sadeghipour and Razi 2000, Correa *et al.* 2005) and vertical confining surfaces (Atmane *et al.* 2003).

Also, the artificial neural network is used for modeling natural cooling of single and multiple horizontal cylinders by Tahavvor and Yaghoubi (2008). This method is also employed by Tahavvor and Yaghoubi (2009; 2011) to simulate the early-stage of frost formation over a cold horizontal cylinder.

From the review of the literature, it can be observed that ANN scheme has rarely employed for natural convection of cold cylinder and an adiabatic plate procedure. Therefore, in this study, a computational procedure based on finite volume method and neural network analysis is used to simulate the free convection heat transfer from a cold horizontal cylinder located above an adiabatic wall. This configuration is used in many industrial applications such as refrigeration industries, chemical industries, power plants, and anywhere which is required to transfer a fluid from one location to another.

## 2. PROBLEM DEFINITION

Figures 1 and 2 show the geometry for a horizontal cylinder above an adiabatic wall surrounded by ambient air, and its grid generated for the CFD in five geometries, respectively. It is obvious that the mesh centralization and compression is around the cylinder and adiabatic plate.

Figure 3 shows the boundary conditions in CFD solution. The temperature of cylinder surface ($T_s$) is assumed to be lower than ambient air temperature

($T_\infty$). Since the flow is symmetric about a vertical plane passing through the center of the cylinder, the half-plane is considered. Therefore, the solution domain is bounded by half of adiabatic wall, half-cylinder surface, lines of symmetry, and the outer boundaries (Fig. 3).
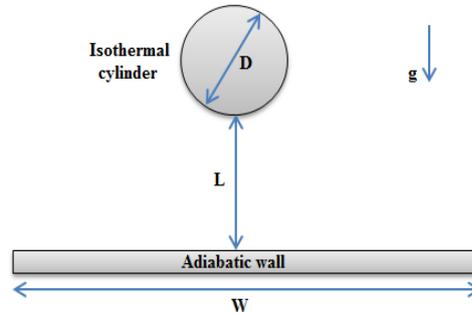


**Fig. 1. Geometry.**

### 2.1 Governing Equations

The governing equations based on Boussinesq approximation for 2D, steady, and laminar free convection around a horizontal cylinder in non-dimensional form are as follows:

$$\frac{\partial}{\partial R}\left(R\frac{\partial\Psi}{\partial R}\right)+\frac{\partial}{\partial\theta}\left(\frac{1}{R}\frac{\partial\Psi}{\partial\theta}\right)=-R\omega \qquad (1)$$

$$\frac{\partial}{\partial R}\left(\omega\frac{\partial\Psi}{\partial\theta}\right)-\frac{\partial}{\partial\theta}\left(\omega\frac{\partial\Psi}{\partial R}\right)=\Pr\left[\frac{\partial}{\partial R}\left(R\frac{\partial\omega}{\partial R}\right)+\frac{\partial}{\partial\theta}\left(\frac{1}{R}\frac{\partial\omega}{\partial\theta}\right)\right]+Ra.\Pr\left(\frac{\partial\emptyset}{\partial R}\sin\theta+\frac{\partial\emptyset}{\partial\theta}\cos\theta\right) \qquad (2)$$

$$\frac{\partial}{\partial R}\left(\emptyset\frac{\partial\Psi}{\partial\theta}\right)-\frac{\partial}{\partial\theta}\left(\emptyset\frac{\partial\Psi}{\partial R}\right)=\left[\frac{\partial}{\partial R}\left(R\frac{\partial\emptyset}{\partial R}\right)+\frac{\partial}{\partial\theta}\left(\frac{1}{R}\frac{\partial\emptyset}{\partial\theta}\right)\right] \qquad (3)$$

where

$$U=\frac{1}{R}\frac{\partial\Psi}{\partial\theta}, V=-\frac{\partial\Psi}{\partial R}, \emptyset=\frac{T-T_s}{T_s-T_\infty}, \omega=\frac{1}{R}\left[\frac{\partial(RV)}{\partial R}-\frac{\partial U}{\partial\theta}\right], \Pr=\frac{\nu}{\alpha}$$

In the above equations, $T_s$ and $T_\infty$ are cylinder surface and ambient temperature respectively. Also, R and θ denote the dimensionless coordinate of the cylindrical coordinate system and Ψ, $\emptyset$, ω, Ra, and Pr are polar stream function, dimensionless temperature, vorticity, Rayleigh number and Prandtl number respectively.

The Boussinesq approximation is defined as:

$$\rho\approx\rho_\infty[1-\beta(T-T_\infty)+\cdots] \qquad (4a)$$

$$\beta=-\frac{1}{\rho}\left(\frac{\partial\rho}{\partial T}\right)_P \qquad (4b)$$

where $\rho_\infty$ and β indicate the ambient density and thermal expansion coefficient respectively.

Governing equations are solved using finite volume method. Average and local Nusselt numbers are defined as follows:
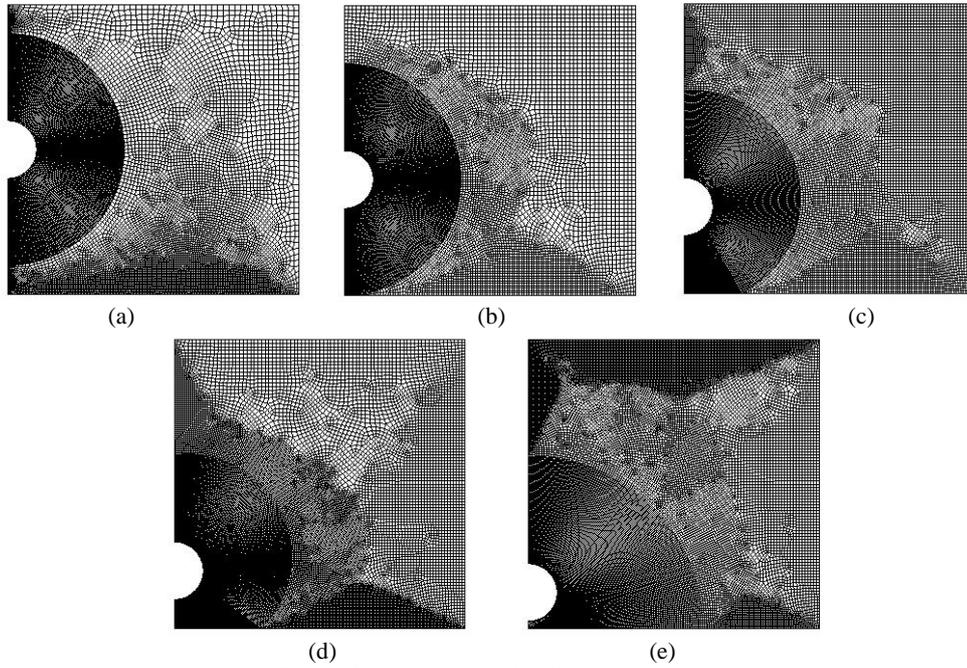
$$Nu_D=\frac{hD}{k} \qquad (5)$$

Fig. 2. Generated grid for five geometries.



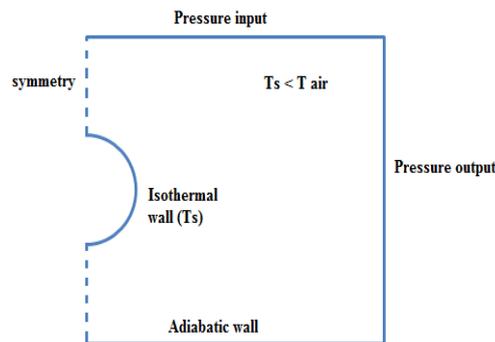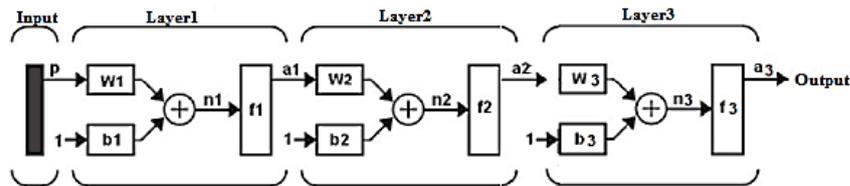Fig. 3. Boundary conditions for CFD simulation.



Fig. 4. Three layer feedforward artificial neural network.

$$\overline{\mathrm{Nu_D}} = \frac{1}{\pi} \int_0^\pi \mathrm{Nu_D}\,(\theta)d\theta = \frac{\overline{q''_{w,D}}\,D}{\Delta T\,k} \tag{6}$$

Where h, D, and k are the convection heat transfer coefficient, cylinder diameter and air thermal conductivity coefficient respectively.

As it is known the flows that appeared because of the density difference that occurred in the case of temperature difference are the free convection flows, and it is occurred in ($10^4 \le \mathrm{Ra} \le 10^8$) for the horizontal cylinders. Hear the problem solved in($10^5 \le \mathrm{Ra} \le 10^7$) by CFD method, in three different Ra's and five different geometries, each one in different distance between cylinder and adiabatic wall. Equation (7) shows the Ra equation

that give us the temperature difference, if thermal diffusivity coefficient (α), kinematic viscosity (ν), and thermal expansion coefficient (β) values are read in film temperature.

$$\mathrm{Ra_D} = \frac{g\beta(T_\infty - T_s)D^3}{\alpha\nu} \tag{7}$$

## 2.2 Boundary Conditions

Boundary conditions are applied on boundaries of model as follows:

- On the symmetry lines: All the normal gradients are equal to zero $\psi = 0, \frac{\partial\psi}{\partial\theta} = 0, \omega = 0$

- On the isothermal cylinder surface: No-slip and No-jump conditions are confirmed $\psi = 0, \emptyset = 0, \omega = -\frac{\partial^2 \psi}{\partial R^2}$

- On the outer region boundary: The pressure constant condition is established, while the pressure assumes the atmospheric one

- On the adiabatic wall: It supposed to be completely insulated $\frac{\partial \emptyset}{\partial \theta} = 0$

## 2.3  Artificial Neural Networks

Artificial neural network (ANN) is a recommended method for complex problems. By using this method, we generalize examples and predict continuation with a high rate. After applying numerical methods, output data's are used as a target for an appropriate neural network. Upon obtaining suitable results for each 15 states by numerical methods, the results are transferred in order to design an integrated new neural network for all range points to ordinary programming software.

Figure 4 shows a view of the network used.

As shown in this figure, the input matrix (p) contains three rows x-coordinate and y-coordinate of the nodes and Ra, which are the numerical results of fifteen desired range of temperatures and locations.  The target matrix (a3) also includes three rows of static temperature and velocity components (T, u, v) corresponding to the input nodes. The weights (w1, w2, and w3) and biases (b1, b2, and b3) are embedded in such a way that the lowest error between the target function and network output are seen. The input and the target have been coded such that the numbers are between zero and one. Thus, the logistic function (f1 and f2) can be used as a sigmoid transfer function in the hidden layers. The neural network used in the project is a three-layer neuron, two hidden layers and an output layer that has benefited from the linear transfer function (f3). It should be noted that after some trial and error, the above network with 15 and 10 neurons in the hidden layers providing the lowest error rate, was accepted. Table 1 shows the network training parameters and its architecture which are used in this study.

**Table 1 ANN architecture and training parameters of neural networks used in this study**

| Number of layers | 3 |
|---|---|
| Activation functions | Input layer: logistic sigmoid Hidden layer: logistic sigmoid Output: linear |
| Number of neuron | Input layer: 10 Hidden layer: 15 Output: 3 |
| Learning rule | Levenberg-Marquardt |
| Learning rule factor | Decreasing: 0.1 Increasing: 10 |
| Mean squared error goal | $10^{-5}$ |

As mentioned before, to study the current project the back-propagation algorithm with Levenberg-Marquardt learning rule was used as it is faster than other functions, uses less memory and has high accuracy. This algorithm is a gradient descent procedure, which is iterative tries to minimize the error criteria such as mean/sum square error between the predicted and desired output. The performance function in the Levenberg-Marquardt method is as follows:

$$F(w) = \sum_{i=1}^{I} \sum_{j=1}^{J} (D_{ij} - A_{ij})^2 \qquad (8)$$

The input argument of function F is the weights and biases. I and J are the number of pattern and number of outputs respectively and $D_{ij}$ and $A_{ij}$ are the desired and actual values of the $i^{th}$ output and $j^{th}$ pattern.

Weights and biases are determined from the following relation:

$$w_{i+1} = w_i - (H + \alpha_i I)^{-1} \nabla F(w_i) \qquad (9)$$

H and I are Hessian and Identity matrix respectively and $\alpha$ is learning parameter. When $\alpha=0$ the Levenberg-Marquardt method tends to Gauss-Newton method and when $\alpha$ is very large the Levenberg-Marquardt method tends to steepest descent algorithm. During the iterative procedure, if the error is decreased, $\alpha$ is decreased (usually by factor 0.1) to reduce the effect of gradient descent and if error is increased, $\alpha$ is increased (usually by factor 10) to follow gradient.

The $R^2$ value can be used or comparison and validation of the neural network results with the numerical method.

$$R^2 = 1 - \frac{\sum(\Omega_{CFD} - \Omega_{ANN})^2}{\sum(\Omega_{CFD} - \Omega_{m,CFD})^2} \qquad (10)$$

Where $\Omega_{CFD}$ the value is determined from CFD computations, $\Omega_{ANN}$ is the obtained value of $\Omega$ from artificial neural network and $\Omega_{m,CFD}$ is the mean value of $\Omega_{CFD}$. The closer this value to 1, the better agreement between these 2 methods could exist. One other value for comparing result of two mentioned methods is Mean Square Error (MSE) that is explained as follows:

$$MSE = \frac{\sum(\Omega_{CFD} - \Omega_{ANN})^2}{number\ of\ nodes} \qquad (11)$$

Results with minimum errors are achieved by applying inputs to different networks and using trial and error. In this procedure iterations start by networks of less layers and neurons, gradually increase number of neurons in hidden layers and then elevate number of layers up to getting the best result. It is evident that from a point onward, the increase in digits will not improve results and even increases the risk of error. Although, it should be noted that networks usually will get closer to an intended error in a logical period of time. If this time increases, it could be understood that from here on no considerable change will be observed in the mentioned network.

Having access to a network with an acceptable error, the $R^2$ value and MSE were calculated to

determine the correlation of the two aforementioned methods. The temperature and velocity profiles can be evaluated or any charting application and compared with the results of CFD.

This geometry can also be used with other Rayleigh numbers (other than three Rayleigh numbers assigned to the network) to realize how practical and comprehensive is the method. To solve the above problem in each distant (L/D) using the neural network, we drafted 5 artificial neural networks for each distant which could be used in predicting flow regime in a whole range of Rayleigh numbers. In this work, the range of variation of Rayleigh numbers is $10^5$ to $10^8$ and about 44000 data were chosen for each Rayleigh number and distance, generated from CFD. Results of each distance were used for training of ANN. It is expected that these five networks be more adaptive with CFD results obtained since they are designed for one and only one specific geometry. In the result part, we will provide a more detailed comparison of these results.

## 3. RESULTS AND DISCUSSIONS

In this study to minimize computational cost and time, one of the soft computation techniques, artificial neural network, is used to determine the flow and temperature domains around a cold horizontal cylinder above an adiabatic wall for different Rayleigh numbers. Obtained results are compared with CFD results. The database for training procedure is generated from a CFD code base on the finite volume method. The behavior fluid around the cold cylinder in free convection have different from the hot cylinder and it has not been studied yet. To achieve this aim following results are presented.

The mentioned problem is solved and analyzed in 15 different cases. To obtain a grid independent solution, various meshes are considered until the total forces of the cylinder almost became constant. The number of cells and nodes of each grid and the results of grid study are presented in Table 2.

**Table 2 The results of grid study on total force exerted on the cylinder**

| L/D | Grid No. 1 # of nodes: 26602 | Grid No. 2 # of nodes: 44336 | Grid No. 3 # of nodes: 70938 |
|---|---|---|---|
| 2/1 | 0.0493049 | 0.0456667 | 0.0451383 |
| 3/2 | 0.0236397 | 0.0229797 | 0.0221327 |
| 1/1 | 0.0205309 | 0.0206524 | |
| 1/2 | 0.0111732 | 0.0110485 | 0.0110085 |
| 1/4 | 0.0061767 | 0.0061195 | 0.0060207 |

The governing equations are solved via SIMPLE technique in order to coupling the pressure and velocity values. Air is chosen as an operating fluid and its properties are considered in standard conditions. The outputs of CFD method are used as

the input and target of the ANN to have an ability of comparing these two methods. Figures 5 thru 9 show the comparison between the temperature profiles around cylinder using two methods.
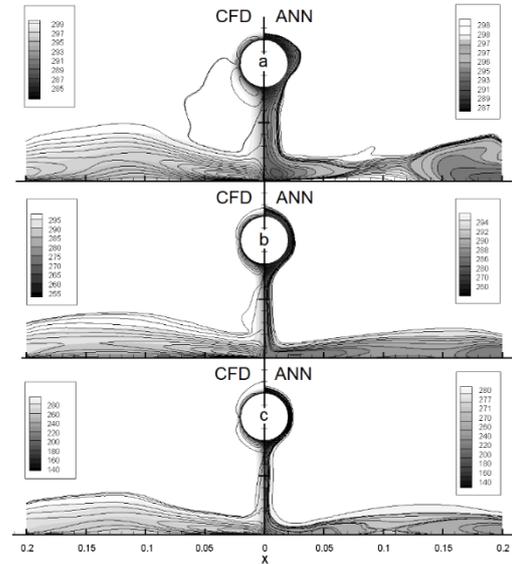


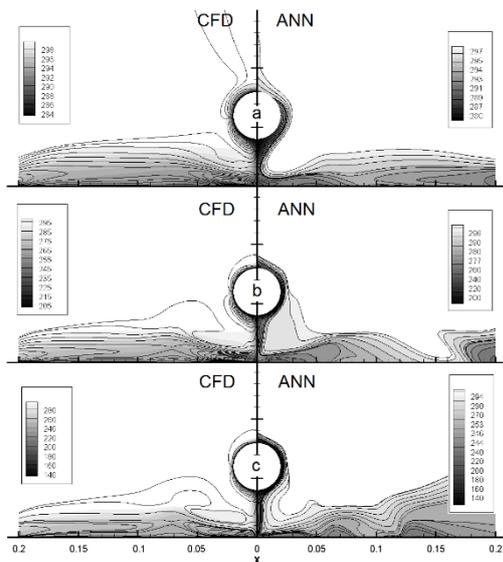**Fig. 5.Temprature distribution for case L/D = 2.0 for (a) Ra = $10^5$, (b) Ra =$2.9 \times 10^5$, and (c) Ra = $10^6$.**
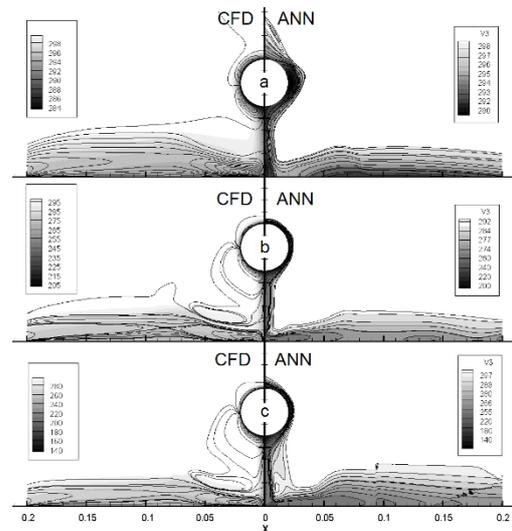


**Fig. 6.Temprature distribution for case L/D = 1.5 for (a) Ra = $10^5$, (b) Ra = $5.8 \times 10^5$, and (c) Ra = $10^6$.**
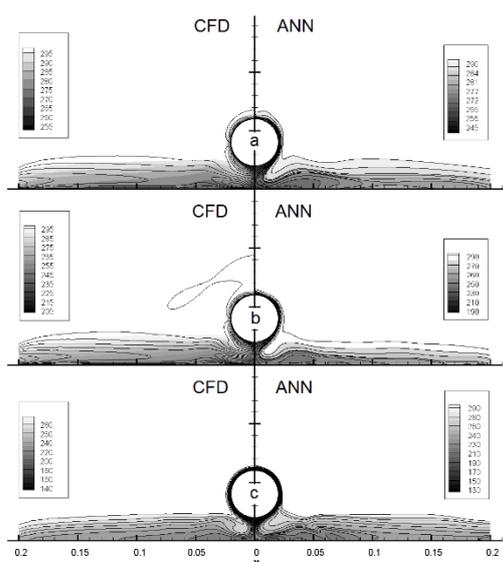
According to the obtained results, downward flow is clear and harmonies of these two methods are verified. By looking at this picture carefully, you'll notice that in lower Rayleigh we see lesser consistency with neural networks, because, in lower Rayleigh, the temperature difference between the cylinder and its environment is very low, thus, node values are very close to each other. The more the cylinder get closer to the adiabatic plate, the stronger vortexes observed below the cylinder. In another word, the separation point occurs at higher angles. The weak vortexes had almost no effect in

streamlines. These vortexes make the local Nusselt number and heat convection coefficient decries in the lower angels of the cylinder.

Table 3 shows the $R^2$ number for all 3 outputs of the networks for each geometry and Table 4 shows it for the general network. Results of comparing two methods have been shown in respective tables. As you can see in Table 3, comparing number $R^2$ shows that for five different designed networks, each for a specific geometry, our expectations have been met efficiently and since it is close to 1 it proves the fact that numerical methods and neural networks, in the study of heat transfer from the cylinder cooler than ambient, have a very good and acceptable compliance with each other.

At the beginning of the study, we expected overall network designed for all five geometry and in all ranges of Rayleigh, which was designed based on 15 different states, would have a good agreement with Computational Fluid Dynamics, but through examining Table 4, we see that this expectation is only partly satisfied. However, it seems that due to the use of different geometries in network design, the results have not gone so well as a network for any geometry.



Fig. 7.Temprature distribution for case L/D = 1.0 for (a) Ra = $10^5$, (b) Ra = $5.8 \times 10^5$, and (c) Ra = $10^6$.



Fig. 8.Temprature distribution for case L/D = 0.5 for (a) Ra = $2.9 \times 10^5$, (b) Ra = $5.8 \times 10^5$, and (c) Ra = $10^6$.
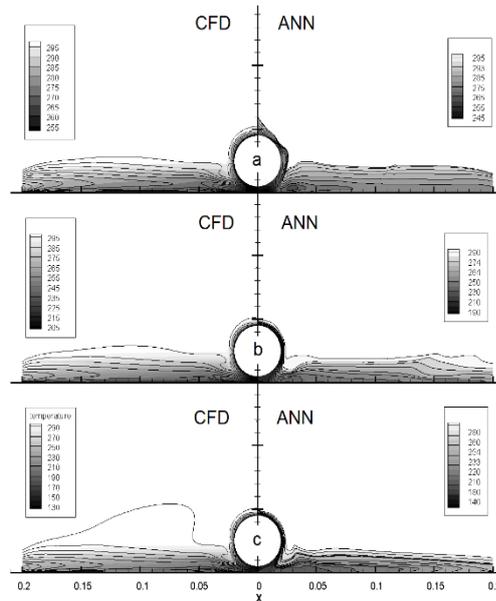


Fig. 9. Temperature distribution for case L/D = 0.25 for (a) Ra = $2.9 \times 10^5$, (b) Ra = $5.8 \times 10^5$, and (c) Ra = $10^6$.

**Table 3 $R^2$ between network target and network outputs for five geometries**

| L/D | Temperature | x-Velocity | y-Velocity |
|-----|-------------|-----------|-----------|
| 2.0 | 0.9227 | 0.9767 | 0.9738 |
| 1.5 | 0.9098 | 0.9690 | 0.9406 |
| 1.0 | 0.9381 | 0.9740 | 0.9753 |
| 0.5 | 0.9870 | 0.9910 | 0.9904 |
| 0.25 | 0.9904 | 0.9607 | 0.9592 |

**Table 4 $R^2$ between targets and network output for general neural network**

|  | Temperature | x-Velocity | y-Velocity |
|--|-------------|-----------|-----------|
| All cases | 0.5943 | 0.7434 | 0.6421 |

It looks like designed networks will benefit from higher degrees of adaptation in case they are designed for one or more close geometries. The more designed geometries are distant from each other, the more decline in the network is possible. In other hand, MSE number is calculated to compare these two methods more operational (Tables 5 and 6).

**Table 5 Mean Square Error for networks in five geometries**

| L/D | Temperature | x-Velocity | y-Velocity |
|-----|-------------|------------|------------|
| 2.0 | $2.1 \times 10^{-5}$ | $6.6 \times 10^{-5}$ | $6.7 \times 10^{-5}$ |
| 1.5 | $3.6 \times 10^{-5}$ | $6.5 \times 10^{-5}$ | $8.9 \times 10^{-5}$ |
| 1.0 | $3.7 \times 10^{-5}$ | $6.4 \times 10^{-5}$ | $5.9 \times 10^{-5}$ |
| 0.5 | $3.3 \times 10^{-5}$ | $5.4 \times 10^{-5}$ | $4.8 \times 10^{-5}$ |
| 0.25 | $9.5 \times 10^{-6}$ | $2.7 \times 10^{-5}$ | $3.1 \times 10^{-5}$ |

**Table 6 Mean Square Error for general neural network**

| | Temperature | x-Velocity | y-Velocity |
|-----|-------------|------------|------------|
| All cases | $6.1 \times 10^{-4}$ | $7.8 \times 10^{-4}$ | $2.8 \times 10^{-4}$ |

Comparing MSE numbers in Table 5 and 6 shows the two methods are really matching with each other, as, the more these numbers are close to zero, the more it indicates coordination of two methods used in the project. Similarly, by comparing the above numbers for the overall designed network which have been shown in Table 4 and 6, we can see these methods are relatively matched, although the results were not as good as an independent network for each geometry.

The average Nusselt number over the cylinder wall is calculated, for the purpose of studying if the adiabatic wall has affected the amount of heat transfer from the isothermal cylinder (Table 7).
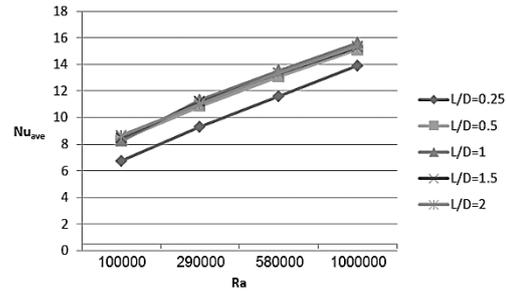
**Table 7 Average Nusselt number**

| L/D | $Ra = 10^5$ | $Ra = 2.9 \times 10^5$ | $Ra = 5.8 \times 10^5$ | $Ra = 10^6$ |
|-----|------------|------------|------------|------------|
| 2.0 | 8.655 | 11.010 | 13.362 | 15.374 |
| 1.5 | 8.454 | 11.181 | 13.314 | 15.300 |
| 1.0 | 8.251 | 11.334 | 13.551 | 15.626 |
| 0.5 | 8.334 | 10.854 | 13.092 | 15.113 |
| 0.25 | 6.749 | 9.318 | 11.592 | 13.886 |

It is obvious that average Nusselt is increases by the increase of Ra and distance L/D. But after L/D=1.5 (in higher distances) the Nusselt become almost constant, so we can assume that the adiabatic wall has no effect in (1.5≤ L/D ≤ ∞). In other word, the affect is renouncement and it works like a cylinder in an infinite environment (Sedaghat *et al*. 2015).

Besides, by increasing the distance of L / D and increasing the Ra, the boundary layer of temperature around the cylinder becomes thinner, therefore increase in the average Nusselt number is occurred which is due to the greater impact of buoyancy forces compared to the viscosity forces. In the lower distances (L / D < 1/2) the alteration of the Nusselt number, become more (sudden decrease) due to the increase of the damping effect of adiabatic wall and dominance in the heat convection around the cylinder. Figures 10 and 11 show the alteration of the average Nusselt number in terms of Ra and L / D based on Table 6.
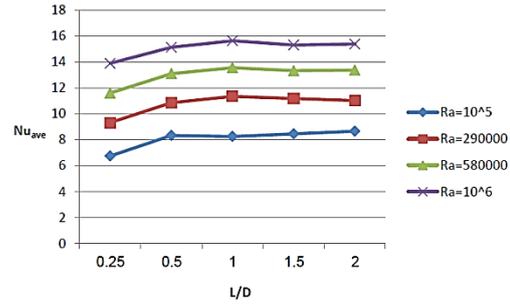


**Fig. 10. Average Nusselt variation for different Rayleigh.**



**Fig. 11. Variation of average Nusselt number for various values of L / D.**

It also obvious that the maximum alteration of the average Nusselt number in each Ra is about 22%. As we consider, the Nusselt in the free convection is affected by Ra or the geometry, hear in constant Ra, changing range of Nusselt is because of geometry.

Two accidental other Ra in order to check the proficiency of the networks in other Ra numbers are entered into the network (Table 8), it shows an excellent agreement between CFD and ANN methods.

**Table 8 Mean Square Error for two accidental Ra**

| | Temp. | x-Velocity | y-Velocity |
|-----|-------|------------|------------|
| $\frac{L}{D} = 2$ $Ra = 4 \times 10$ | $6.5 \times 10^{-4}$ | $5.2 \times 10^{-2}$ | $5.1 \times 10^{-3}$ |
| $\frac{L}{D} = 0.5$ $Ra = 7 \times 10$ | $2.4 \times 10^{-3}$ | $7.0 \times 10^{-2}$ | $6.2 \times 10^{-2}$ |

It's clear that we can trust in the neural networks in predicting the outputs in all range of Ra number.

It is also be noted that to simulate the prescribed problem, a PC with a CPU of Intel(R) 2.0 GHz and installed memory 8.0 GB is used. With this configuration, each CFD simulation takes a time of about four hours. ANN training, due to a large amount of training data, takes a time of about 14 hours. But after the training procedure, the ANN weights and biases are tuned and network learns and capture the behavior of flow and obtaining results from ANN for any other Rayleigh number take a time less than 10 seconds. Therefore, artificial neural networks save computational time considerably.

## 5. CONCLUSION

Results from one of soft computations techniques, artificial neural networks, is compared with numerical results for simulation of free convection heat transfer from a cold cylinder above an adiabatic plate in $10^5 \leq Ra \leq 10^8$.

Results indicate that:

- Excellent agreement was found between ANN results and numerical results in the 5 cases network designing for every special distance.

- Back-propagation algorithm with Levenberg-Marquardt learning rule is the best choice for training this type of ANNs because of the accurate and faster training procedure and less computer space usage.

- Artificial neural networks can be used fluently to determine flow and temperature domain in free convection cooling with considerably less computational time and cost.

- Free convection from the cold cylinder is categorized as aiding flow while from the hot cylinder is categorized as opposing flow, therefore the behavior of these situations are different from each other.

- The more the cylinder get closer to the adiabatic plate, the stronger vortexes observed below the cylinder as the separation point is occurred in higher angles.

- When Rayleigh number increases, due to an enhancement of buoyancy force in comparison to the viscous force, the thermal and velocity boundary layers become thinner.

- In lower Rayleigh, less agreement between neural networks and CFD solution is observed, since in lower Rayleigh the temperature difference between the cylinder and its environment is very low and as a result, node values are very close to each other and round-off errors play an important role.

- More average Nusselt number reduction takes place when the cylinder is closer to the adiabatic plate; owing to an enhancement of plate damping effect.

- In spaces farther than L / D = 3/2, the average Nusselt number is almost constant, so the effect is renouncement and it works like a cylinder in an infinite environment.

## REFERENCES

Ashjaee, M., A. Eshtiaghi, M. Yaghoubi and T. Yousefi (2007). Experimental investigation on free convection from a horizontal cylinder beneath an adiabatic ceiling. *Experimental Thermal and Fluid Science* 32, 614-623.

Atayılmaz S.O., H. Demir, and Ö. Ağra (2010). Application of artificial neural networks for prediction of natural convection from a heated horizontal cylinder. *International Communications in Heat and Mass Transfer* 37(1), 68-73.

Atmane, M. A., V. S. S. Chan and D. B. Murray (2003). Natural convection around a horizontal heated cylinder: the effects of vertical confinement. *International Journal of Heat and Mass Transfer* 46(19), 3661-3672.

Correa, M., R. Parra, A. Vidal, J. Rodriguez, M. Aguilera and D. Gonzalez (2005). Natural convection around a horizontal cylinder near an adiabatic cover wall. *Proceeding of Fourth ICCHMT*, 336.

Firat, M. and M. Goungor (2007). River flow estimation using adaptive neuro-fuzzy inference system. *Math. Compute. Simulation* 75, 87–96.

Hasiloglu, A., M. Yilmaz, O. Comakli and I. Ekmekci (2004). Adaptive neuron-fuzzy modeling of transient heat transfer in circular duct air flow. *Int. J. Therm. Sci.* 43, 1075–1090.

Lawrence, G., G. Jardin, D. Naylor and A. Machin (1999). Free convection from a horizontal heated cylinder located below a ceiling. *Transactions of the Canadian Society for Mechanical Engineering* 23, 19-35.

MCculloch, W. S. and W. Pitts (1990). A Logical Calculus of the Ideas Immanent In Nervous Activity. *Bulletin of Mathematical Biology* 52(1), 99-115.

ÖzgürAtayılmaz, S., H. Demir and O. Ağra (2010). Application of artificial neural networks for prediction of natural convection from a heated horizontal cylinder. *International Communications in Heat and Mass Transfer* 37, 68–73.

Sadeghipour, M. S. and Y. P. Razi (2000). Natural convection from a confined horizontal cylinder: the optimum distance between the confining walls. *International Journal of Heat and Mass Transfer* 44, 367-374.

Saito, T, R. Ishiguro and Y. Fujishima (1969). Natural convection heat transfer around a horizontal cylinder (effect of a horizontal plate placed above the cylinder). *Proceeding of 6th National Heat Transfer Symposium*. Japan.

Sedaghat, M. H., M. Yaghoubi M and M. J. Maghrebi (2015). Analysis of natural convection heat transfer from a cylinder enclosed in a corner of two adiabatic walls. *Experimental Thermal and Fluid Science* 62, 9-20.

Tahavvor, A. R. and M. Yaghoubi (2008). Natural cooling of horizontal cylinder using artificial neural network (ANN). *International Communication in Heat and Mass Transfer* 35, 1196-1203.

Tahavvor, A. R. and M. Yaghoubi (2011). Prediction of frost deposition on a horizontal

circular cylinder under natural convection using artificial neural networks. *International journal of refrigeration* 34, 560-566.

Tahavvor, A. R., and M. Yaghoubi (2009). Analysis of early-stage frost formation in natural convection over a horizontal cylinder. *International Journal of Refrigeration* 32, 1343-1349.

Temeyer, B. R., W. A. Gallus, K. A. Jungbluth, D. Burkheimer and D. McCauley (2003). Using an Artificial Neural Network to predict parameters for frost deposition on Iowa bridge ways. *Proceedings of the Mid-Continent Transportation Research Symposium*, Iowa, USA, 1-6. Iowa State University.

Thibault, J. and P. Bernard (1991). A neural network methodology for heat transfer data analysis. *Heat mass transfer* 34(8), 2063-2070.

Varol, Y, E. Avci, A. Koca and H. F. Oztop (2007). Prediction of flow fields and temperature distributions due to natural convection in a triangular enclosure using Adaptive-Network-Based Fuzzy Inference System (ANFIS) and Artificial Neural Network (ANN). *Int. Community. Heat Mass Transfer* 34, 887–896.

Yamamoto, S., D. Niiyama and B. R. Shin (2004). A numerical method for natural convection and heat conduction around and in a horizontal circular pipe. *International Journal of Heat and Mass Transfer* 47, 5781–5792.